Optical reflectivity and carrier localization in incommensurate misfit layer compounds $(MS)_xTaS_2$ (M = rare-earth metal, Pb, Sn)

Kazuya Suzuki
Department of Chemistry, Yokohama National University, Hodogaya-ku, Yokohama 240, Japan

Toshiaki Enoki
Department of Chemistry, Tokyo Institute of Technology, Meguro-ku, Tokyo 152, Japan

Hiroyuki Tajima
Department of Chemistry, The University of Tokyo, Bunkyo-ku, Tokyo 113, Japan
(Received 6 July 1995)

The optical reflectance spectra of incommensurate misfit layer compounds $(MS)_xTaS_2$ (M=rare-earth metal, Pb, Sn) were measured in the range of 3.1 to 0.093 eV and were analyzed by the Drude-Lorentz model. The spectra show clear Drude edges whose energies were significantly lowered from that of the host material 2H-TaS_2. The charge transfer from MS to TaS_2 was estimated on the basis of the rigid-band model. We found that the effective mass of carriers in the TaS_2 conduction band depended on the degree of charge transfer from MS to TaS_2, which was explained by the modification of the electronic structure from a two-carrier to a one-carrier system with respect to the degree of charge transfer. The degree of charge transfer depending on rare-earth elements is related to the modification of the band structure of MS due to the lattice incommensurability between the MS and TaS_2 sublattices, which is the most peculiar nature of $(MS)_xTaS_2$.

I. INTRODUCTION

Recently, structural and physical properties of incommensurate misfit layer compounds $(MX)_xTX_2$(M=Pb, Sn, Bi, and rare-earth elements; T=Ti, V, Cr, Nb, and Ta; and X=S and Se) have been studied intensively.[1,2] These compounds have quite a rare crystal structure consisting of MX layers and TX_2 layers stacked alternately. The MX slab forms a double layer whose structure is derived by slicing the pristine MX with the rocksalt structure along the [00l] direction. The TX_2 slab is a well-known layered structure comprising the hexagonal X-T-X sandwich layers. A stacking structure of $(MX)_xTX_2$ is shown in Fig. 1. Since the crystal structures of the two pristine compounds MX and TX_2 have different lattice symmetries and their basic structures are preserved in the formation of the alternative stacking, $(MX)_xTX_2$ exhibits lattice misfit between the MX and TX_2 layers. As a consequence the lattice constants in one in-plane direction are independent between the two sublattices, and the ratio of the lattice constant becomes irrational (incommensurate) in this direction. Such incommensurate characteristics have been found in the electron-diffraction spectra. The electron-diffraction pattern of $(MX_x)TX_2$ consists of the superposition of the reflections from the distorted hexagonal TX_2 layers and the distorted tetragonal MX layers, and satellite reflections are usually observed along the incommensurate direction as a result of the mutual lattice modulation.

In the TaS_2-based compounds with rare-earth metal (R) sulfides, $(RS)_xTaS_2$, the transport properties such as electrical resistivity, thermoelectric power, Hall effect, and magnetoresistance indicate that the conduction carriers exist predominantly in the TaS_2 layer, while the carriers in the RS layer, which still exist after the electron transfer from RS to TaS_2, do not take part in the electrical conduction.[3–5] Both the pristine compounds RS and TaS_2 have one conduction electron per unit cell. Therefore if the composition ratio x in $(RS)_xTaS_2$ in unity, and the conduction electron in the RS band is completely

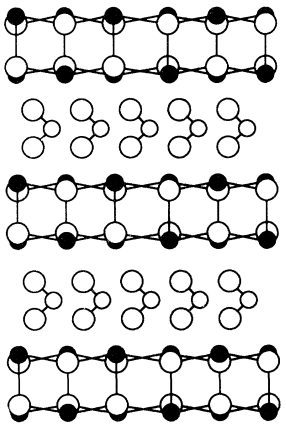

FIG. 1. Stacking structure of $(MX)_xTX_2$ projected along the a-axis. M: filled circle; X: large open circle; and T: open small circle. The MX double layer and the TX_2 sandwich layer stack alternately.

transferred to the TaS_2 band, then $(RS)_xTaS_2$ becomes insulating. In $(RS)_xTaS_2$, the ratio of the lattice parameters between the RS and TaS_2 sublattices is irrational, then x is also irrational. This means that any degree of charge transfer cannot make the system insulating, because some amount of conduction electrons should remain in the TaS_2 and/or RS conduction bands. In addition, because of the facts that the parameter x is larger than unity, and TaS_2 can accept one electron at the most, conduction electrons *do* remain in the RS layers. The inconsistency between the prediction from the band-structure consideration and experimental findings has been resolved by an idea of carrier localization in RS layers due to the quasiperiodic potential associated with the lattice incommensurability.[5] The fact that the VS_2-based compounds $(RS)_xVS_2$ are semiconducting provides evidence for the above idea, in which the conduction electrons in the VS_2 conduction band are also localized as well as those in the RS conduction band. It was recently discovered that the quasiperiodic potential can make the electronic system localized,[6–9] so that if we know the degree of charge transfer from RS to TaS_2 we can show what kind of quasiperiodicity forms in $(RS)_xTaS_2$. We performed optical reflectivity measurements for $(MS)_xTaS_2$ (M=Pb, Sn, La, Ce, Nd, Sm, Gd, Dy, Er, and Yb) in order to evaluate the carrier densities from the plasma frequencies of the free-carrier-like reflectivity. In this paper, we present the reflectance spectra and discuss the relation between the lattice incommensurability and the electronic structure of $(MS)_xTaS_2$.

II. EXPERIMENTS

Crystals suitable for reflectivity measurements were prepared by a chemical transport method using iodine as a transport agent. Mixed element powders in the ratios corresponding to their chemical composition were heated in an evacuated silica tube with iodine (5 mg per reaction volume) at a temperature gradient of 950–850 °C. Crystals were grown in lamellar and ployhedral shapes whose dimension was up to 5 mm in a side, and thickness less than 50 μm. Well-crystallized samples were obtained by using MS or M_2S_3 as starting materials instead of the constituent elements.

Polarized reflectance spectra were taken at room temperature by a microspectrophotometric technique in the wave numbers 750–25 000 cm^{-1} (0.093–3.1 eV) using Olympus MMSP-RK between 4200 and 25 000 cm^{-1} (0.52 and 3.1 eV) and Jasco MIR-300 IRD between 750 and 4200cm^{-1} (0.093 and 0.52 eV). Samples were cleaved by adhesive tapes to obtain flat and clean surfaces, and mounted on the sample holder together with the tape used for cleaving. Spectra were taken on the (001) crystal surfaces in the polarization direction parallel to the b axis (the commensurate direction within the layer). Single-crystal silicon was used for a standard to estimate absolute reflectivity.

III. RESULTS

Figure 2 shows the polarized reflectance spectra of $(SmS)_{1.19}TaS_2$ taken at room temperature between 0.093 and 3.1 eV in the polarization direction parallel to the b axis. Rotation of the polarization direction within the basal plane does not change the reflectivity beyond experimental accuracy. The reflectivity of $(SmS)_{1.19}TaS_2$ has a minimum at around 0.58 eV, which is a clear Drude edge consistent with the metallic nature of this compound. Above the Drude edge, the reflectivity rises with energy with slight humps at around 0.9 and 2.3 eV, and reaches 35% at 3.1 eV. These humps in the reflectance spectra are due to interband transitions. Such outstanding features are common in $(MS)_xTaS_2$ measured here, although their Drude edges are slightly different from each other. The reflectance spectra of 2H-TaS_2 have similar

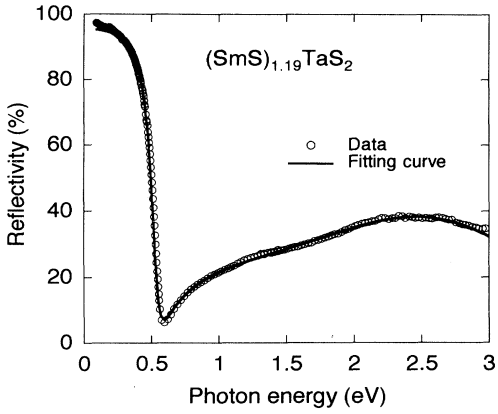

FIG. 2. The optical reflectivity of $(SmS)_{1.19}TaS_2$ (open circle) and a fitting curve (solid line) to the Drude-Lorentz model (Sec. IV).

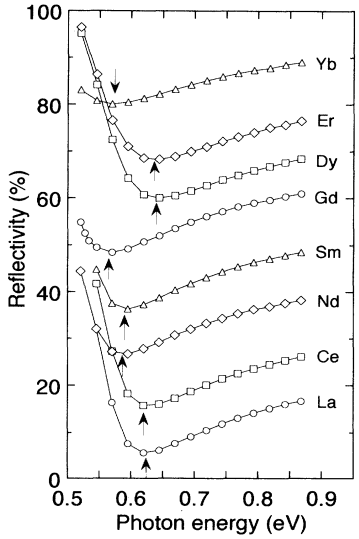

FIG. 3. The optical reflectivity of $(RS)_xTaS_2$ plotted around the Drude edges (0.5–0.9 eV). For clarity, the curves are shifted upward by every 10% from R = La to Yb. The arrows show the reflectivity minimum corresponding to the Drude edge. Note that the energy of the reflectivity minimum drops from R = La to Gd rises to Dy, then drops again.

features. After Parkin and Beal,[10] the Drude edge in the reflectance spectra of 2H-TaS_2 locates at around 1.35 eV, and above the Drude edge two interband transitions are found with well-defined peaks at 3.3 and 5.5 eV. The reflectivity minimum corresponding to the Drude edge in $(MS)_xTaS_2$ is significantly lowered from the Drude edge of 2H-TaS_2. The differences in the energies of the Drude edges and the interband transitions between 2H-TaS_2 and $(MS)_xTaS_2$ are related to the difference of the carrier density as a result of the electron transfer from the MS layer to the TaS_2 layer.

Figure 3 is the reflectance spectra of $(RS)_xTaS_2$ in the variation of R in the range of 0.5–1 eV. In the higher-energy region above the Drude edge, the reflectivity of the measured compounds shows quite a similar energy dependence. This fact indicates that the contributions of the interband transitions in this energy region and those of the low-energy tails of the interband transitions at much higher energies are almost the same in these compounds. Therefore it is considered that the interband transitions in the RS layers will not make a significant contribution to the reflectance spectra, and the origin of the spectra can be assigned to that from TaS_2. As seen in Fig. 3, the Drude edges differ slightly among the $(RS)_xTaS_2$ compounds. Increasing the atomic number of R, the Drude edge first drops from R=La to Gd, then rises stepwise at R=Dy, and then drops again. Since the transport properties of $(RS)_xTaS_2$ are almost identical, and are dominated by the conduction carriers on the TaS_2 layers, their Drude edges are ruled by the carrier density in the TaS_2 conduction band, namely by the degree of charge transfer from MS to TaS_2. The rare-earth dependence of the Drude edge will be discussed in Sec. IV in terms of the charge transfer and carrier localization.

Figure 4 is the comparison of the reflectance spectra among $(SnS)_{1.16}TaS_2$, $(PbS)_{1.13}TaS_2$, $(LaS)_{1.13}TaS_2$, and $(GdS)_{1.20}TaS_2$. The energies of the Drude edges for the Sn and Pb compounds are detected at around 0.8 eV, which values are larger by about 0.3 eV than those for the rare-earth compounds. This result directly indicates the low electron transfer from SnS or PbS to TaS_2. Since the pristine SnS and PbS are semiconducting with the valence states of Sn^{2+} and Pb^{2+}, charge transfer is not expected so much as in $(RS)_xTaS_2$. The low electron transfer in the Sn and Pb compounds are suggested by transport properties[2,11] because of the similarity to those of pristine 2H-TaS_2. Their Hall coefficients show a strong temperature dependence, and the thermoelectric power is negative in contrast to $(RS)_xTaS_2$. Above the Drude edges, the reflectivity rises with a convex curvature to 50% at 3.1 eV, which exceeds the reflectivity of 2H-TaS_2 at the same energy. This means a significant contribution of the interband transition in the SnS or PbS layer. In addition, a small peak was found at around 1.8 eV. This peak, between the Drude edge and the first well-defined interband transition peak, is commonly found among the Vb-transition-metal dichalcogenides, at 2.1 eV for 2H-TaS_2,[10] 1.5 eV for NbS_2[12] and 1.8 eV for 2H-$TaSe_2$.[13]

The reflectivity of the TaS_2-based misfit layer compounds $(PbS)_{1.13}TaS_2$, $(LaS)_{1.13}TaS_2$, and $(SmS)_{1.19}TaS_2$ was recently reported by Rüscher *et al.*[14] The reflectance spectra of these three compounds are in good agreement with our results. The reflectivity of the NbS_2-based compounds[14–16] is also quite reminiscent of that of the TaS_2-based compounds, except that the energy of the Drude edge is slightly lower.

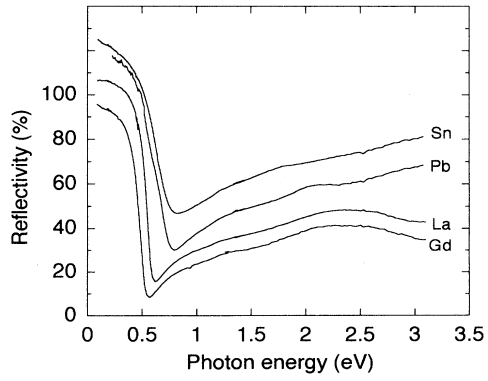

FIG. 4. Comparison of the optical reflectivity among $(GdS)_{1.20}TaS_2$, $(LaS)_{1.13}TaS_2$, $(PbS)_{1.13}TaS_2$, and $(SnS)_{1.16}TaS_2$. For clarity, the curves are shifted upward by every 10% in this order. Note that energy of the Drude edge and the reflectivity beyond the Drude edge in the Sn and Pb compounds are higher than in the rare-earth compounds.

IV. DISCUSSION

A. Band structure of $(MS)_xTaS_2$ and Drude-Lorentz fitting

Before fitting the reflection spectra to some theories, we consider an appropriate model describing the electronic structure of $(MS)_xTaS_2$. The band structure of 2H-TaS_2 calculated by Mattheiss[17] is illustrated in Fig. 5. The valence band consists mainly of sulfur 3p-orbital character, as denoted by p. The conduction bands are mainly formed of the Ta 5d orbital slightly mixed with the S 3p orbital, which are split by the trigonal crystal field into the lowest lying d_{z^2} and d (p), respectively.

As we pointed out in our previous papers,[3,5] the electrical conduction in $(MS)_xTaS_2$ is dominated by the conducting hole carriers on the TaS_2 layer alone. The conduction carriers on the MS layers are localized due to the quasiperiodic potential associated with lattice incommensurability. Therefore the contribution of the carriers in the MS band to the reflectance spectra is renormalized into the constant dielectric function term because the optical scattering time is much smaller than in the TaS_2 band. Thus the free-carrier-like reflectivity comes from the carriers in the TaS_2 conduction-band as mentioned in Sec. III. In the single-carrier Drude model, the complex dielectric function is represented by

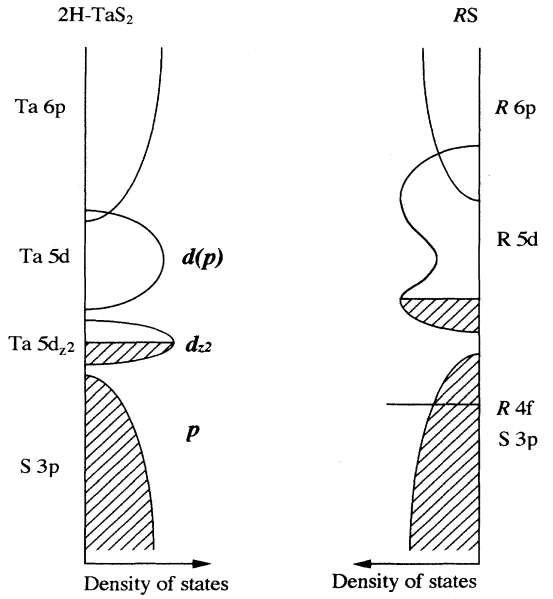

FIG. 5. Schematic band picture of 2H-TaS_2 and *RS*. The principal orbitals that construct each energy band are also shown. The valence and conduction bands of 2H-TaS_2 are denoted as p, d_{z^2}, and $d(p)$. Electrons in the conduction band of *RS* (with *R* a 5*d* character) are transferred to the vacancy of the d_{z^2} band.

$$\varepsilon_D = -\frac{\omega_p^2}{\omega^2 + i\gamma\omega} , \tag{1}$$

where ω_p and γ are the plasma frequency and relaxation rate for the free carriers, respectively. According to the band calculations for 2H-TaS_2,[17] there are at least two Fermi surfaces in the conduction band, so that it is necessary to use more than one Drude component for fitting. This model, however, is not worthwhile for the present case because the reflectance spectra do not have any marked structures around the Drude region. Namely, even if we employ $\Sigma\omega_{p,i}^2$ instead of ω_p^2 in Eq. (1), it is difficult to determine each $\omega_{p,i}$ accurately.

The high reflectivity above the Drude edge arises from interband transitions. Parkin and Beal[10] have pointed out that the interband transitions in 2H-TaS_2 in this energy region are those from the valence p band to upper conduction $d(p)$ band [p-$d(p)$ transition] and from the half-filled d_{z^2} band to the upper conduction band [d_{z^2}-$d(p)$ transition], whose resonance energies are 5.5 and 3.3 eV, respectively. Within the measured energy region in our experiments (<3.1 eV), it is enough to take the latter transition into account for the theoretical fitting, and the effect of the p-$d(p)$ transition is renormalized into the constant dielectric term.

A small hump in the reflectance spectra at 1.8 eV for the Sn and Pb compounds can be assigned to the interband transition from the high density-of-states region in the valence p band to the unfilled portion of the d_{z^2} band (p-d_{z^2} transition), as assigned for pristine 2H-TaS_2.[10] This transition strongly depends on charge transfer from *MS* to TaS_2. The increase of the charge transfer makes the d_{z^2} band fill up, then the p-d_{z^2} transition shifts to higher energy and the oscillator strength is reduced significantly. Therefore the p-d_{z^2} transition is absent in $(RS)_x TaS_2$ because of the large charge-transfer rate.

The similarity of the spectra above the Drude edge among $(RS)_x TaS_2$ indicates that the interband transitions originate from the TaS_2 layer and that those from the *RS* layer do not contribute to the reflectance spectra. It is considered that the interband transitions in the *RS* part require higher energies than the measured energy region, so that the contribution is renormalized in the frequency-independent dielectric constant term. The interband transition in the *RS* part was found in the isostructural compounds $(CeS)_x NbS_2$ ($x=0.6$ and 1.) (Ref. 15) as a small hump centered at 3.1 eV.

Taking the above notion into consideration, all the reflectance spectra are fitted to the following theoretical model consisting of frequency-dependent contributions to the dielectric constant, a Drude term from free carriers, that from interband transitions described by one Lorentzian oscillator where *M* is a rare-earth metal or two oscillators for *M* = Sn and Pb, and a frequency-independent contribution from the core term. The complex dielectric constant is given by

$$\varepsilon = \varepsilon_c + \varepsilon_D + \varepsilon_L \tag{2}$$

and

$$\varepsilon_L = \sum_j \frac{B_j^2}{\omega_{0j}^2 - \omega^2 - i\Gamma_j\omega} , \tag{3}$$

where ε_c is the contribution from the core transition and tails of high-energy interband transitions excluding the Lorentzian oscillator taken here. ε_L is the dielectric constant of the Lorentz term with the resonant frequency ω_0 and the damping factor Γ. The parameter B is related to the Lorentzian oscillator strength A as $A=(B/\omega_0)^2$. Summation is taken for the p-d_{z^2} and d_{z^2}-$d(p)$ transitions. The vertical reflectivity is given by

$$R = \frac{(n-1)^2+k^2}{(n+1)^2+k^2} , \tag{4}$$

where n is the reflactive index and k is the extinction coefficient, which are related to the real and imaginary parts of the dielectric constants ε_1 and ε_2 as

$$n^2 = \tfrac{1}{2}[(\varepsilon_1^2+\varepsilon_2^2)^{1/2}+\varepsilon_1] , \tag{5}$$

$$k^2 = \tfrac{1}{2}[(\varepsilon_1^2+\varepsilon_2^2)^{1/2}-\varepsilon_1] . \tag{6}$$

The fitting parameters are summarized in Table I, and a typical fitting curve is drawn in Fig. 2 by a solid line. One can find that the theoretical fitting to the data is quite satisfactory, so that it is proved that the model consisting of one Drude and one or two Lorentz components is enough for the present analysis. Based on this analysis,

TABLE I. Energy at the reflectivity minimum $\hbar\omega_{min}$ and optical fitting parameters for $(MS)_xTaS_2$ [see Eqs. (1–3)], frequency-independent dielectric constant ε_c, plasma frequency ω_p, carrier scattering rate γ, Lorentzian oscillator resonance frequency ω_0, and Lorentzian oscillator damping factor Γ. B is a parameter of the Lorentzian oscillator related to the Lorentzian oscillator strength A as $A=(B/\omega_0)^2$.

M	$\hbar\omega_{min}$ (eV)	ε_c	$\hbar\omega_p$ (eV)	$\hbar\gamma$ (eV)	$\hbar\omega_0$ (eV)	$\hbar\Gamma$ (eV)	$\hbar B$ (eV)	A
La	0.62	3.2	1.71	0.043	2.22	1.22	5.11	5.30
Ce	0.63	3.2	1.72	0.062	2.23	1.30	5.17	5.37
Nd	0.59	3.2	1.64	0.038	2.22	1.34	5.29	5.68
Sm	0.58	3.2	1.61	0.055	2.26	1.19	5.43	5.77
Gd	0.56	3.2	1.59	0.056	2.17	1.14	5.40	6.19
Dy	0.64	3.2	1.71	0.052	2.23	1.18	4.99	5.00
Er	0.63	3.2	1.71	0.052	2.21	1.15	5.17	5.47
Yb	0.57	3.2	1.53	0.087	2.26	1.19	5.26	5.42
Pb	0.80	3.7	2.44	0.087	2.74	1.24	6.68	5.94
					1.98	0.495	1.83	0.85
Sn	0.83	3.2	2.54	0.180	2.70	1.24	7.44	7.59
					2.11	0.433	1.96	0.86

we discuss the electronic structures and charge transfers in $(MS)_xTaS_2$ in the following subsections.

B. Interband transition

Because of the identical reflectance spectrum among the rare-earth compounds $(RS)_xTaS_2$, the fitting parameters of the Lorentz term and the core term are almost the same values, namely $\hbar\omega_0 \sim 2.2$ eV, $\hbar\Gamma \sim 1.2$ eV, $\hbar B \sim 5$ eV, and $\varepsilon_c \sim 3.2$. As previously mentioned, this interband transition is assigned to eh d_{z^2}-$d(p)$ transition in the TaS_2 part, which corresponds to the reflectivity maximum at 3.3 eV in the pristine 2H-TaS_2. In $(RS)_xTaS_2$, electrons are transferred from RS to TaS_2, and fill the d_{z^2} band by more than half. Therefore, in the d_{z^2}-$d(p)$ transition, the charge transfer causes the increase of the oscillator strength by increasing the electron density in the d_{z^2} band, the decrease in the threshold resonance energy by the upshift of the Fermi energy and the increase of the width in the Lorentz term.

Such a pronounced redshift of the interband transition energy is known in the lithium intercalation compounds $Li_xTaS_2 (0<x\leq 1)$.[18] In the completely intercalated compound $LiTaS_2$, the color of the crystal changes from metallic blue of 2H-TaS_2 to transparent orange-red as a result of the full charge transfer. The reflectivity maximum due to the d_{z^2}-$d(p)$ transition shifts from 3.3 to 2.5 eV and the transition width is considerably broadened. In addition to the decrease of the threshold resonance energy by charge transfer, Guo and Liang pointed out in their band calculation for Li_xTaS_2 (Ref. 18) that the charge transfer increases the energy of the d_{z^2} band. Therefore, the charge transfer causes the decrease in the energy gap between the d_{z^2} and $d(p)$ bands to make the resonance energy of the d_{z^2}-$d(p)$ transition lower.

The Lorentzian oscillator strength in the d_{z^2}-$d(p)$ transition defined as $A=(B/\omega_0)^2$ depends on rare-earth elements, as seen in Table I. The oscillator strength A increases with the atomic number of the rare-earth element from R = La to Gd, discontinuously decreases at R = Dy, and then increases again. A possible contribution from the RS part to the reflectivity in this energy region is the interband transition from S $3p$ valence band to R $5d$ conduction band. It is known that the onset energy of the S $3p$–R $5d$ transition is at around 3.3 eV, and is almost independent of R.[19,20] Therefore the contribution of the interband transition in the RS part may not give significant rare-earth dependence of the oscillator strength. One can see in Table I that the trend of the rare-earth dependence of the oscillator strength A is opposite to the trend of the plasma frequency ω_p. As already mentioned, the oscillator strength of the d_{z^2}-$d(p)$ transition depends on the number of electrons accommodated in the d_{z^2} band. With increasing charge transfer from RS to TaS_2, the conduction hole carrier decreases, while the number of electrons in the d_{z^2} band increases. Since ω_p^2 is proportional to the conduction hole carrier density, the opposite relation between A and ω_p in the rare-earth dependence is a natural corollary. Thus the trend of the oscillator strength A is ascribed to the difference of the charge-transfer rate among the rare-earth compounds.

Figure 4 shows clear differences of the reflectivity in the interband transition region among $(RS)_xTaS_2$, and $(PbS)_{1.13}TaS_2$, and $(SnS)_{1.16}TaS_2$. The reflectivity of $(PbS)_{1.13}TaS_2$ and $(SnS)_{1.16}TaS_2$ is much higher than in the rare-earth compounds, and even exceeds that of 2H-TaS_2. Because of the low electron transfer rate from SnS or PbS to TaS_2, the electronic structures of the valence and conduction bands in $(PbS)_{1.13}TaS_2$ and $(SnS)_{1.16}TaS_2$ are quite analogous to the pristine one, giving rise to the similar reflectance spectra. In addition to the d_{z^2}-$d(p)$ transition, there is a weak structure at around 1.8 eV for both of the compounds. This peak can be assigned to the p-d_{z^2} transition in the TaS_2 part. In the same energy region, there may be a transition between the valence (S $3p$) and conduction (Sn $5p$ or Pb $6p$) bands in the MS part.

The direct energy gap in the α and β-SnS is estimated at 1.4 eV by optical-absorption measurements,[21] and 1.4~1.8 eV by band calculations.[22] These values denote the onset of the transitions, so that the resonance energy that characterizes the interband transition may be much higher because of the wide energy bandwidths in both the valence and conduction bands. The effect of the interband transition in the MS part will contribute at the higher-energy region, resulting in a higher reflectivity than in 2H-TaS_2. This is clearly found in Table I as the oscillator strength is much larger than in the rare-earth compounds.

C. The Drude region: Electron transfer in $(MS)_xTaS_2$

From fitting parameters in the Drude component, we can estimate density, Fermi energy, and optical conductivity by using a model consisting of a two-dimensional cylindrical Fermi surface and quadratic energy dispersion. The carrier density n_c is proportional to the square of the plasma frequency as

$$\omega_p^2=\frac{4\pi n_c e^2}{m^*}=\frac{4\pi e^2}{m_e}\frac{n_c}{p} , \tag{7}$$

where m^* is the effective mass of the carriers, m_e is the free-electron mass, and $p=m^*/m_e$. The Fermi energy E_F is related to the carrier density n_c as

$$E_F=\frac{\pi\hbar^2 I_c}{m^*}n_c , \tag{8}$$

where I_c is the distance between adjacent TaS_2 layers. In connection with Eq. (7), E_F is simply obtained from the relation

$$\omega_p^2=\frac{4e^2}{\hbar I_c}E_F . \tag{9}$$

The optical conductivity is calculated by the formula

$$\sigma_{op}=\frac{n_c e^2\tau}{m^*}=\frac{\omega_p^2\tau}{4\pi} . \tag{10}$$

In Table II the obtained values of E_F, n_c, and σ_{op} are shown with I_c, the composition ratio x in $(RS)_x$ TaS_2 and observed dc conductivity σ_{dc}.

The Fermi energies of $(RS)_xTaS_2$ are not different from each other. If the effective mass is the same at any wave vectors within the conduction band, the carrier density n_c is proportional to the Fermi energy for the two-dimensional electronic system. From Table II, E_F depends on R elements, but differs only by 20% between the La and Gd compounds.

Using the direct relation between the plasma frequency and carrier density [Eq. (7)], and assuming that the effective mass is equal to the free-electron mass m_e ($p=1$), the carrier density is tentatively obtained as $n_c=0.236$ for La and 0.193 for Gd compounds. In contrast, the carrier density n_c estimated from Hall-effect measurement is very different in each $(RS)_xTaS_2$; for example, hole carriers per TaS_2 are 0.12 for $R=$La (Ref. 2) and 0.04 for $R=$Gd.[2,4] Even taking into account the experimental errors in the Hall-effect measurements, the disagreements between the carrier density estimated from the optical and that from transport measurements are quite large. Therefore, it is considered that such disagreements are intrinsic, and may come from the difference in the effective masses of carriers.

Only for 2H-$NbSe_2$ do we know the effective mass of the conduction carrier $m^*=1.4m_e$ among 2H-polytype transition-metal dichalcogenides.[10] If we tentatively use this value for the effective mass in $(RS)_xTaS_2$, the carrier density is further increased, and the disagreements are enhanced. Therefore, to align the carrier densities obtained by the two measurements, the effective mass must be much reduced from that of the pristine 2H-TaS_2.

TABLE II. Chemical composition ratio x in $(MS)_xTaS_2$, interlayer distance of adjacent TaS_2 layers I_c, Fermi energy E_F, carrier density per TaS_2 measured by the Hall effect n_{RH}, n_c/p defined in Eq. (7), effective-mass ratio $p=m^*/m_e$, optical scattering time τ, optical conductivity σ_{op}, and dc conductivity σ_{dc}.

M	x	I_c (Å)	E_F (eV)	n_{RH}[a,b]	n_c/p	p	$\tau(10^{-14}$ s)	σ_{op}(S cm^{-1})	σ_{dc}(S cm^{-1})[a,c]
La	1.13	11.51	0.57	0.12	0.236	0.51	1.51	9.2×10^3	4.2×10^3
Ce	1.14	11.45	0.57	0.14	0.232	0.60	1.17	6.4	4.8
Nd	1.16	11.36	0.53	0.10	0.210	0.48	0.82	9.5	2.9
Sm	1.19	11.27	0.54	0.05	0.198	0.25	1.18	6.3	3.2
Gd	1.20	11.25	0.50	0.04	0.193	0.21	0.96	6.1	1.9
Dy	1.22	11.18	0.57	0.09	0.222	0.41	1.17	7.6	4.3
Er	1.23	11.12	0.56	0.09	0.219	0.41	1.17	7.6	4.8
Yb	1.23	11.10	0.46		0.174		1.96	3.6	
Pb	1.13	11.98	1.00	0.48	0.495		1.96	9.2	6.2
Sn	1.16	11.88	1.11	1.62	0.529		4.08	4.8	3.1

[a]Reference 2.
[b]Reference 4.
[c]Reference 3.

When we adopt the carrier density measured by the Hall coefficient, the effective masses are estimated at $m^*=0.51m_e$ for La and $0.21m_e$ for Gd compound. These values are reduced by $\sim\frac{1}{3}$ and $\sim\frac{1}{6}$ from the effective mass of the pristine compounds, respectively. Such a great reduction of the effective mass from the pristine compounds has been found by Terashima *et al.* for $(CeS)_{1.2}NbS_2$,[15] and by Parkin and Beal for 3*d*-transition-metal intercalation compounds.[10] They referred the origin of the reduced effective mass to interlayer interactions that cause the conduction bandwidth to broaden. The interlayer interaction in TaS_2 originates from the direct S-S contact between the adjacent TaS_2 layers.

Recent band calculations for some TaS_2-intercalation compounds showed negative conclusions as to the further broadening of the d_{z^2}-band-width after intercalation. For $LiTaS_2$,[18] because of the weak mixing of the S 3*p* orbital and the Li 2*S* orbital, the interlayer interaction does not have an effect on the d_{z^2} band. The d_{z^2} band tends to be narrower due to the increase in the interlayer distance of TaS_2. For the cases of $Mn_{1/3}TaS_2$ and $Fe_{1/3}TaS_2$,[23] the 3*d* states of Mn and Fe strongly hybridize with the 5*d* states of Ta, but the TaS_2 partial density of states is quite similar to that of the host 2H-TaS_2. Therefore the intercalation of some metallic species modifies the dispersion of the d_{z^2} band just a little. It is mentioned that the covalency bonds between the *M* and S atoms (in the TaS_2 layer) are formed in actual, but the hybridization is quite weak in $(MS)_xTaS_2$. Therefore we consider that the hybridization effect between *M*S and TaS_2 does not modify the dispersion curves of the TaS_2 d_{z^2} band.

Here we refer to the significant modification of the band structure of TaS_2 by the insertion of *M*S. The enhancement of the interlayer separation between adjacent TaS_2 layers modifies the structure of the conduction band of TaS_2 to some extent. In Mattheiss's calculation, the d_{z^2} band consists of the two energy dispersions because there are two TaS_2 molecules in the unit cell. In the limit of the two-dimensional energy band, the energy dispersion along $\Gamma MK\Gamma$ and that along *ALHA* are the same as shown in Fig. 6, where the dispersion curve has two peaks at the symmetric points Γ and *K* with nearly equal energies. Mattheiss also mentioned that the wave function at the Γ point is formed mainly of the Ta $5d_{z^2}$ orbital, while at the *K* point the Ta $5d_{x^2-y^2}$ and $5d_{xy}$ orbitals mainly construct the wave functions. Therefore, the character of the wave function depends on where the Fermi energy intersects the dispersion curve of the d_{z^2} band.

This effect is of significance in $(RS)_xTaS_2$ because the conduction hole carriers are located at the top of the d_{z^2} band. Since the energies of the d_{z^2} band at the Γ and *K* points differ only a little, $(RS)_xTaS_2$ has two types of hole carriers with the wave vector at around the Γ and *K* points. Increasing the degree of charge transfer, the Fermi energy rises, and the d_{z^2} band becomes almost filled; then only one type of hole carriers at around the highest peak of the d_{z^2} band takes part in the electrical conduction. Since the wave functions differ between the *K* and Γ points, it is possible to differ the effective masses between these two types of carriers. At the *K* point, the wave functions, d_{xy} and $d_{x^2-y^2}$, extend within the layers and are therefore not affected by interlayer interactions. In contrast, the d_{z^2} orbital is affected significantly by interlayer interactions that broaden the bandwidth. Therefore, it is considered that the carriers at the former point have heavier effective masses. This situation is accomplished in $(RS)_xTaS_2$. By changing *R* from La to Gd, the degree of charge transfer is increased, and the portion of heavier carriers is decreased.

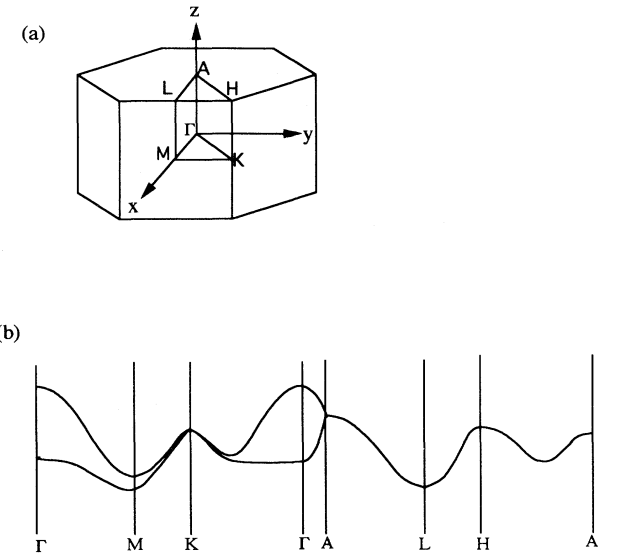

FIG. 6. The first Brillouin zone (a) and the dispersion curves of the d_{z^2} band (b) for 2H-TaS_2. In the two-dimensional limit, the dispersion curves along $\Gamma MK\Gamma$ degenerate and are coincident to that along *ALHA*. In $(RS)_xTaS_2$, the Fermi energy is located at the top of the d_{z^2} band.

This is supported by the experimental results of the magnetoresistance.[5] The magnetoresistance of $(RS)_xTaS_2$ at liquid-He temperatures, and the carrier density estimated from the Hall coefficient n_{RH} shows quite a similar rare-earth dependence. For instance, the magnetoresistance at $H=5$ T is 1.4% for the La compound, and decreases with atomic number of rare-earth metals to 0.4% for the Gd compound. Since the magnetoresistance originates from the presence of multicarriers having different effective masses, the variation of the magnetoresistance as a function of rare-earth metal suggests that the portion of one type of carriers decreases more rapidly than another type of carriers with decreasing total carrier densities. This fact is consistent with the rare-earth dependence of the effective mass considered above.

The carrier densities for $(PbS)_{1.13}TaS_2$ and $(SnS)_{1.16}TaS_2$ were estimated to be 0.50 and 0.53, assuming $m^*=m_e$. We do not compare these carrier densities

and those obtained by Hall effects, because the latter were derived on assuming a one-carrier system.[11] According to the literature, the Hall coefficient shows a significant temperature dependence, and presumably a magnetic-field dependence is present. This fact suggests that at least two carriers with different effective masses and opposite signs exist.

According to the x-ray photoemission and x-ray-absorption measurements,[24–26] the spectra are interpreted in terms of the simple superposition of the spectra of TaS_2 and PbS or SnS, so that the interlayer interaction is inferred to be quite small. In these papers, Ohno[24] showed some evidences of the presence of small charge transfer, while Ettema and co-workers[25,26] concluded that there is no charge transfer from PbS or SnS to TaS_2. If the charge transfer does not occur, the effective mass of the conducting carrier is estimated at $m^*=2.0m_e$, which is the same result with that reported by Rüscher *et al.*[14] The effective mass of $2.0m_e$ is considerably larger than that of the pristine 2H-TaS_2. The enhanced effective mass may be attributed to the narrowing of the d_{z^2} conduction band of TaS_2 due to the lack of interlayer interactions.

D. Carrier localization in $(RS)_xTaS_2$

Here we refer to the carriers in the MS layer that should remain after charge transfer. Figure 7 is a plot of the Fermi energy in $(RS)_xTaS_2$ as a function of rare-earth elements. The Fermi energy at first decreases with increasing the atomic number of R up to $R=$Gd, then increases at $R=$Dy and finally decreases again. The trend of E_F in the variation of R is reminiscent of the trend on n_{RH} measured by the Hall effect, although the variation rate is much larger in E_F than in n_{RH}. As has been discussed,[5] the carriers in the RS conduction band are localized due to the quasiperiodic potential associated with the lattice incommensurability. In the incommensurate direction in the crystal (the crystallographic a direction), conduction electrons remaining in the conduction band of RS undergo an additional quasiperiodic potential from TaS_2 layers. If the two sublattices are really incommensurate throughout the crystal, the energy gaps appear in the a^* direction, the density of states of the conduction band at the energies where the zone folding takes place becomes lower than that of pristine RS. If the Fermi energy is located at the energy, the carrier localization is likely to occur by additional random potentials because of the low density of states. This may be the main reason why the carriers in the RS band are localized. Based on the above, we propose that the number of remaining electrons in the conduction band of RS after charge transfer is related to the ratio of the lattice constants in the incommensurate direction, namely $r=a_{RS}/a_{TaS2}$. Here a schematic illustration of the density of states after zone folding in shown in Fig. 8. The remaining electron in the RS conduction band is denoted in this figure as a shaded region, which we call a subband.

The composition ratio x in $(RS)_xTaS_2$ is equal to $1/2r$. Therefore, with increasing atomic number of R, the composition ratio x increases monotonically because the lattice parameter of pristine RS decreases with the atomic number of R. This fact suggests that the charge transfer governed by r changes monotonically with x, and, accordingly, the Fermi energy estimated from the plasma frequency also changes monotonically with x. Contrary to the above discussion, the Fermi energy and n_{RH} estimated by experiments show discontinuous change between $R=$Gd and Dy, or at around $x\sim1.2$, as seen in Fig. 7. This experimental fact indicates that the remaining electron in the RS conduction band is different between the cases $x<1.2$ and $x>1.2$.

Such a variation of E_F is probably justified by the presence of the discommensurate structure. The composition ratio x lies in the range $1.13<x<1.23$, corresponding to

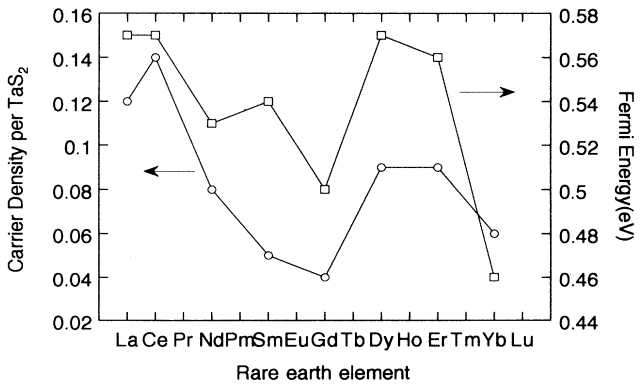

FIG. 7. Plot of E_F (right scale) and n_{RH} (left scale) as a function of rare-earth elements. The lines are a guide for the eye. Note that the both parameters show a discontinuous change between $R=$Gd and Dy.

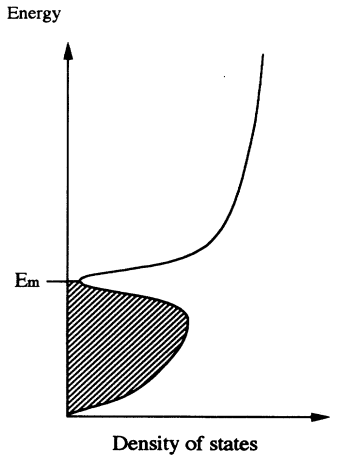

FIG. 8. Two-dimensional band scheme with a one-dimensional quasiperiodic potential. The zone-folding effect causes a minimum in the density of states at $E=E_m$, where the zone folding takes place in the incommensurate direction.

$1.755 > r > 1.612$. Some simple rational numbers close to r are $\frac{7}{4}, \frac{5}{3}, \frac{8}{5}$, etc. The composition ratio $x = 1.2$ corresponds to the ratio of the two sublattices $r = \frac{5}{3}$, therefore the discontinuous change of E_F at $x \sim 1.2$ is related to the formation of a three-folded superlattice in the RS sublattice and five-folded superlattices in the TaS_2 sublattice. Then the conduction band of RS forms a subband by the three-folded superlattice.

Here we consider that the electrons above the subband are transferred to TaS_2. In this case, the number of the remaining electrons, which are accommodated in the subband, is independent of x when the three-folded sublattice is formed. Then the number of the transferred electrons per RS is the same for any value of x, while the transferred electron per TaS_2 is proportional to x. This is the case for $x < 1.2$. The increase of E_F at $R = \mathrm{Dy}$ in Fig. 7 with increasing atomic number of R means that more hole carriers are present in the TaS_2 conduction band for $x > 1.2$ than for $x < 1.2$, and hence the number of the remaining electron in the RS conduction band is larger than in the case of $x < 1.2$ As to the possible discommensurate structure for the case $x > 1.2$, it is considered that the next simple ratio of the two sublattices r is $\frac{8}{5}$. In this case, a five-folded superlattice in the RS sublattice is presumably formed for $x > 1.2$ instead of the three-folded superlattice for $x < 1.2$.

This idea is also supported theoretically. It is obvious that if r is rational as $r = n/m$ (n, m; integer), mth-folded structure opens energy gaps in the conduction band. In the case that r is very close but not equal to n/m, Nakano and Machida[27] have shown that the energy gaps open at the same energies for the case of mth-folded structure, and in addition, intragap states also appear. Therefore, the main energy gap depends on the number m where r is approximated as n/m.

The presence of the discommensurate structure is very likely to occur in $(RS)_xTaS_2$. The satellite diffraction spots found in the electron-diffraction pattern along the a^* direction are an evidence of the mutual lattice modulation of the two sublattices. Wiegers and Meershaut[2] mentioned that the lattice modulation in the RS sublattice occurs more strongly than in the TaS_2 sublattice. To release the local stress associated with the lattice misfit between the two sublattices RS and TaS_2, each constituent atom in the RS layer tends to move a more stable position than that in the lattice-misfit situation. As to the high-resolution electron microscopic image, Kuypers *et al.*[28] found in $(SnS)_{1.17}NbS_2$ that the images consist of a set of three or four bright points and dark lines appearing alternately along the incommensurate direction. They have discussed such an arrangement in the images very strictly, taking into account experimental conditions and effect of stacking faults and have shown the possibility of the superstructures present in $(SnS)_{1.17}NbS_2$. In addition, it has been remarked that covalent bonds between R in the RS layer and S in the TaS_2 layer are built in the compounds,[29] although the net interlayer interaction is still weak. The presence of such covalent bonds depends intensely on the relative position of R and S; therefore, the rare-earth atoms tend to move to the positions preferable to form covalent bonds. Therefore, the presence of a discommensurate structure is inevitable for $(RS)_xTaS_2$.

E. Optical conductivity

Finally we comment on the optical conductivity calculated from Eq. (3) an listed in Table II. The optical conductivity σ_{op} is directly related to the plasma frequency ω_p and optical scattering time τ. In comparison with the dc conductivity σ_{dc}, the optical conductivity is in the same order of magnitude but about twice as large as σ_{dc} for almost all of the compounds. As in the dc conductivity, the optical conductivity does not show a schematic rare-earth dependence. This fact supports the conclusion from the dc conductivity that the magnetic moment does not affect the conductivity in $(RS)_xTaS_2$, and the conduction electron in the RS part does not take part in the electrical conduction. Discussion of the difference in absolute value of the conductivity between σ_{op} and σ_{dc} is not worthwhile because σ_{op} is intrinsically not the same as σ_{dc}. We may, however, infer that the difference between σ_{op} and σ_{dc} comes from the difference in the carrier mobility. In addition to the carrier scattering rate $1/\tau$ estimated from the optical reflectance spectra, the carrier scattering rate involved in σ_{dc} is affected by the domain boundaries, lattice imperfections, impurity potentials, and so on. Taking into account these carrier scatterings, the observed conductivities by two types of measurements are well cosistent with each other.

V. CONCLUSION

In this paper, we report the optical reflectivity for $(MS)_xTaS_2$, where M represents rare earth elements, and Pb and Sn are measured between 0.093 and 3.1 eV.

The reflectivity shows a free-electron-like spectrum whose Drude edge is significantly lowered in comparison with the pristine compound 2H-TaS_2. The carrier density was derived from the Drude-Lorentz fitting. In comparison with the carrier density estimated from the Hall effect, we found that the effective mass of the conduction carrier strongly depends on the rare-earth elements, although the plasma frequency is fairly the same. This fact is accounted for in terms of the specific character in the TaS_2 conduction band, in which the electronic system changes from two-hole-carrier conduction with quite different effective masses to one-hole-carrier conduction with a very light effective mass by decreasing the carrier density in the TaS_2 conduction band.

We also discussed the carrier localization due to the quasiperiodic potentials associated with the lattice incommensurability, which is the most specific feature of this type of compound. The quasiperiodic potential forces the one-dimensional energy gap in the incommensurate direction and forms a subband in the RS conduction band. The number of electrons accommodated in the subband (remaining in the RS conduction band after charge transfer) varies with respect to the chemical composition ratio, $x < 1.2$ and $x > 1.2$. It is concluded that the x dependence is related to the formation of the superstructure locally; in other words to the formation of the

discommensurate structure. The superstructure characterizing the discommensuration corresponds to the three-folded superstructure in the RS sublattice for R from La to Gd ($1.13 < x 1.2$), and the five-folded superstructure from Dy to Yb compounds ($1.2 < x < 1.23$). This type of carrier localization is essentially caused by the presence of lattice incommensurability and quasiperiodic potential. Thus, this study provides evidence of the electron localization by quasiperiodic potentials in actual compounds.

[1]G. A. Wiegers, A. Meetsma, S. van Smaalen, R. J. Haange, J. Wulff, T. Zeinstra, J. L. de Boer, S. Kuypers, G. Van Tendeloo, J. Van Landuyt, S. Amelinckx, A. Meerchaut, P. Rabu, and J. Rouxel, Solid State Commun. **70**, 409 (1989).
[2]G. A. Wiegers and A. Meershaut, Mater. Sci. Forum **100&101**, 101 (1992), and references are therein.
[3]K. Suzuki, T. Enoki, and K. Imaeda, Solid State Commun. **78**, 73 (1991).
[4]K. Suzuki, T. Kondo, and T. Enoki, Mol. Cryst. Liq. Cryst. **245**, 43 (1994).
[5]K. Suzuki, T. Enoki, and S. Bandow, Phys. Rev. B **48**, 11 077 (1993).
[6]S. Aubry and G. André, Ann. Isr. Phys. Soc. **3**, 133 (1980).
[7]D. R. Hofstadter, Phys. Rev. Lett. **51**, 1198 (1983).
[8]M. Kohmoto, L. P. Kadanoff, and C. Tang, Phys. Rev. Lett. **50**, 1870 (1983).
[9]S. Ostlund and R. Pandit, Phys. Rev. B **29**, 1394 (1984).
[10]S. S. P. Parkin and A. R. Beal, Philos. Mag. **42**, 627 (1980).
[11]J. Wulff, A. Meetsma, S. van Smaalen, R. J. Haange, J. L. de Boer, and G. A. Wiegers, J. Solid State Chem. **84**, 118 (1990).
[12]A. R. Beal and W. Y. Liang, Philos. Mag. **33**, 121 (1976).
[13]A. R. Beal and S. Nulsen, Philos. Mag. B **43**, 985 (1981).
[14]C. H. Rüscher, C. Haas, S. van Smaalen, and G. A. Wiegers, J. Phys. Condens. Matter **6**, 2117 (1994).
[15]T. Terashima, N. Kojima, H. Kitagawa, H. Okamoto, and T. Mitani, J. Phys. Soc. Jpn. **62**, 2166 (1993).
[16]M. Hangyo, T. Nishio, S. Nakashima, Y. Ohno, T. Terashima, and N. Kojima, Jpn. J. Appl. Phys. **32**, 581 (1993).
[17]L. F. Mattheiss, Phys. Rev. B **8**, 3719 (1973).
[18]G. Y. Guo and W. Y. Liang, J. Phys. C **20**, 4315 (1987).
[19]P. Wachter, Phys. Rep. **44**, 159 (1978).
[20]A. N. Gusatinskii, G. I. Aleperovich, and A. V. Soldatov, Phys. Status Solidi B **112**, 559, (1982).
[21]W. Albers, J. Appl. Phys. **32**, 2220 (1961); M. Parenteau and C. Carlone, Phys. Rev. B **41**, 5227 (1990).
[22]A. R. H. F. Ettema, R. A. de Groot, C. Haas, and T. S. Turner, Phys. Rev. B **46**, 7363 (1992).
[23]J. Dijkstra, P. J. Zijlema, C. F. van Bruggen, C. Haas, and R. A. de Groot, J. Phys. Condens. Matter **1**, 6363 (1989).
[24]Y. Ohno, Phys. Rev. B **44**, 1281 (1991).
[25]A. R. H. F. Ettema, C. Haas, and T. S. Turner, Phys. Rev. B **47**, 12 794 (1993).
[26]A. R. H. F. Ettema and C. Haas, J. Phys. Condens. Matter **5**, 3817 (1993).
[27]M. Nakano and K. Machida, Phys. Rev. B **33**, 6718 (1986).
[28]S. Kuypers, G. Van Tendeloo, J. Van Landuyt, and S. Amelinckx, Acta. Crystallogr. Sec. A **45**, 291 (1989).
[29]A. R. H. F. Ettema, Ph.D. thesis, University of Groningen, 1993.